Online Estimation of Point-based Volumetric Stiffness Model Using Joint Torque Sensors

Shaoxiong Yao[1] and Kris Hauser[1]

***Abstract*—This paper introduces a method for learning the force response of novel, heterogeneous deformable objects directly from robot sensor data without prior knowledge. We present a new volumetric stiffness field representation and a point-based collision dynamics model that lends itself to rapid estimation using force or torque measurements. By estimating the stiffness of each colliding point using an extended Kalman filter, our method can update a stiffness field over a grid of 8 million cells at 17Hz. Experiments show that for the task of predicting the force response from a robot with joint torque sensors repeatedly touching parts of an artificial plant, our method is more accurate than other learning methods by a wide margin.**

I. Introduction

Robots deployed in domestic [1] and agricultural [2] environments must frequently interact with deformable objects like clothes and plants. Although it is relatively well known how to plan paths and manipulation trajectories if a deformable object model is assumed [3, 4], it is far less clear how to estimate a model of the deformable object in the first place. Various deformable object models have been used in robotics applications [5]. Material parameter identification methods are available to match observed deformation or force/torque data to FEM [6] or spring-mass models [7]. However, they are computationally expensive and assume a given mesh topology. Tactile models based on machine learning methods predict the force response at varying touch locations, and avoid strong assumptions about the mesh structure [8, 9]. However, these prior works assume a roughly planar object, discrete touches, and coherence in the object's force response across the object's surface.

Inspired by the problem of plant manipulation, our method addresses deformation modeling for highly heterogeneous objects and continuous movement through a volume. We propose a *volumetric stiffness field* (VSF) model where the object's potential resistance to movement is represented by points anchored to cells on a voxel grid. The stiffness of each Hookean spring is treated as an unknown distribution and estimated by our algorithm. As the robot arm sweeps across voxels, a fast point-based simulator estimates how the points are displaced by the arm, and an extended-Kalman filter estimator updates the stiffness distribution as a function of force or torque measurements. Similar probabilistic methods have been used to estimate the locations of rigid contacts from torque measurements [10, 11], and similar volumetric methods have been used to map the shape of rigid objects from contact [12, 13]. Compared to these methods, the VSF model has two important features:

- Independence between points allows efficient realtime estimation;
- Flexibility to represent objects with heterogeneous stiffness, e.g. plants with hard branches and soft leaves.

We test our method in a scenario in which a robot arm touches an artificial plant. Our method updates the belief of a volumetric stiffness field with 8 million voxels at 17 Hz. The estimated stiffness field is used to predict joint torques when the same location is touched multiple times, and despite the simplicity of the point-based dynamics model, our method is approximately 10 times more accurate than learning-based approaches. Moreover, the estimated stiffness fields qualitatively identify stiffer regions like branches from softer regions like leaves, which has applications to tactile modeling of general deformable objects.

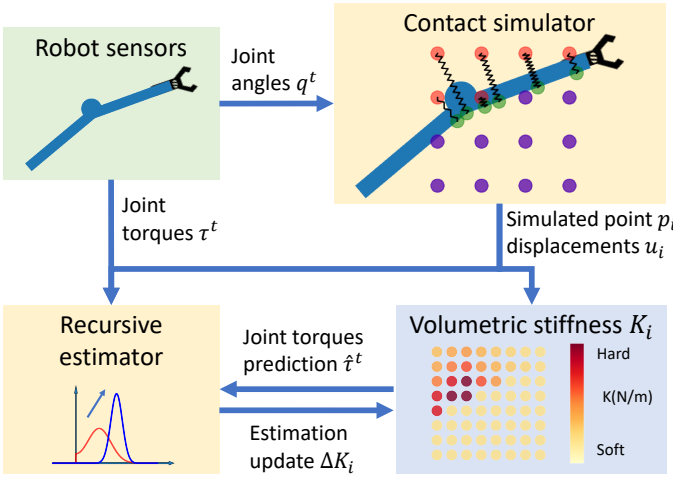

Fig. 1. Our volumetric stiffness field (VSF) estimation system consists of: (1) a contact simulator that simulates the displacement of points pushed by the robot arm, (2) a VSF containing estimated stiffness distributions, (3) a recursive state estimator that updates the VSF beliefs.

II. Method

The VSF models a deformable object as a set of points $\{p_i\}_{i=1..N}$ from a region W expressed in a world frame. When the robot arm sweeps through W, some subset of points will be displaced by the arm. We denote the indices of contact points as $W_c \subset \{1, .., N\}$ and the displacement of point p_i at time t as $u_i^t \in \mathbb{R}^3$. The model makes three key assumptions on the displacements and force responses:

[1]: S. Yao and K. Hauser are with the Department of Computer Science, University of Illinois at Urbana-Champaign, IL, USA. {syao16, kkhauser}@illinois.edu

(i) Hookean force response. Each point has a virtual spring with stiffness $K_i \in \mathbb{R}_+$ connecting it to its rest position p_i. The force response F_i^t at time t is:

$$F_i^t = -K_i \cdot u_i^t \tag{1}$$

(ii) Quasi-static, stick-slip motion. We assume the robot arm moves slow enough such that points move quasi-statically, and points in contact can either stick to the arm or slip along the surface of the arm;

(iii) Independent motion. We assume there is no interaction between points, and the belief over of the stiffness coefficient of each point is independent ($P(K_i, K_j) = P(K_i)P(K_j)$ for $i \neq j$);

This last assumption is the most restrictive compared to mass-spring and FEM models, but as we shall see it allows us to perform estimation of the stiffness field extremely quickly and is a reasonable approximation for some objects. Also note that we make no distinction between empty and occupied space; with a properly estimated VSF, a point p_i in empty space should have stiffness $K_i = 0$.

At each time step, we sequentially step the contact simulator, query the VSF, and update the VSF using a recursive estimator. Firstly, the contact simulator will update the contact set W_c^t and displacements u_i^t given the new arm configuration q^t. Then, using u_i^t and K_i^t, the volumetric stiffness field will predict force response F_i^t for $i \in W_c$. The joint torques τ^t will be a low-dimensional linear observation of F_i^t as well as K_i^t. Finally, the recursive estimator will update the belief of K_i^t.

Contact simulator: The contact simulator receives the robot arm's current configuration q^t at every time step. It also maintains an internal state of contact points W_c^{t-1} and displacements $\{u_i^{t-1}\}_{i \in W_c^{t-1}}$ in the previous time step. Because of the independence assumption (iii), the simulator will update the state of each point in parallel. The simulator simulates three effects: (1) contact detection by distance threshold δ, (2) stick motion with friction coefficient μ, (3) slip motion in tangential direction with fixed step λ. Here δ, μ and λ are the hyper-parameters of the simulator. The simulator performs constant-time updates to each point and the time complexity is bounded by $O(|W_c^t|)$.

We assume the robot arm moves quasi-statically (ii), so the external torques τ can be obtained by subtracting the gravitational torques from total torques. The relation between joint torques and force responses is given by:

$$\tau^t = \sum_{i \in W_c^t} J(q^t, p_i + u_i^t)^\top F_i^t, \tag{2}$$

where $J(q^t, p_i + u_i^t)$ is the contact Jacobian matrix that maps joint velocity to the translational velocity at $p_i + u_i^t$.

Recursive estimator: Our goal is to have a probabilistic estimation of $K_i \in \mathbb{R}^+$. Because the stiffness is non-negative, we cannot use a Gaussian belief which has support for negative values. We reparametrize the stiffness as observation of a hidden state $K_i = |\kappa_i|$, and $\kappa_i \in \mathbb{R}$ is unconstrained. The belief of each κ_i is Gaussian:

$$\kappa_i \in \mathcal{N}(\mu_{\kappa_i}, \sigma_{\kappa_i}^2) \tag{3}$$

(a) Configuration 1 (b) Configuration 2

Fig. 2. Two configurations of the robot arm touching the same location with the same end-effector pose.

Because of the independence assumption (iii), the belief of each κ_i is independent, which means $P(\kappa_i, \kappa_j) = P(\kappa_i) \cdot P(\kappa_j)$ if $i \neq j$. It means we do not need to update a full covariance matrix that correlates the stiffness estimation at different points.

To perform a Bayesian update of the belief, we need a transition model of κ_i and an observation model of τ^t. We assume a static transition model with growing uncertainty:

$$\kappa_i^{t+1} = \kappa_i^t + \epsilon_\kappa, \tag{4}$$

where $\epsilon_\kappa \sim \mathcal{N}(0, \sigma_\kappa^2)$.

We also assume there is independent Gaussian noise $\epsilon_\tau \sim \mathcal{N}(0, \sigma_\tau^2 I)$ in torque measurements at every time step. Combining equations 1 and 2, we have

$$\tau^t = -\sum_{i \in W_c^t} J(q^t, p_i + u_i^t)^\top u_i^t |\kappa_i^t| + \epsilon_\tau \tag{5}$$

Because the absolute value function makes the observation function non-linear, we use an extended-Kalman filter (EKF) to estimate stiffness coefficients. The observation matrix H_t can be derived by linearizing 5 and each column of H_t equals to $\partial \tau^t / \partial \kappa_i^t$,

$$\frac{\partial \tau^t}{\partial \kappa_i^t} = -J(q^t, p_i + u_i^t)^\top u_i^t \cdot \text{sgn}(\kappa_i^t) \tag{6}$$

In practice, we find the EKF may make inaccurate torques prediction at previous configurations. We maintain a buffer of EKF observation matrices H^t and observed τ^t. At each step, after we update the filter with current observation, we will uniformly draw a fixed number of past measurements and do normal Kalman update using sampled past measurement sequentially. We find this technique can mitigate the problem that filter forgets past observations, which also improves torque prediction accuracy on a test sequence.

III. Experiments

We performed a real-world experiment using a Kinova Gen3 robot arm touching an artificial plant. We consider the case where W is a box centered at the arm base with dimensions $2.4m \times 2.4m \times 2.4m$, which fully contains reachable region by the arm. We uniformly discretize this box into a grid with 200^3 points and the distance between neighbor points is $1.2cm$.

A. Stiffness estimation for torque prediction

We first evaluate whether an estimated VSF can accurately predict joint torques when the same location is touched but a different configuration. Fig. 2 shows the robot arm touches

TABLE I
TORQUE PREDICTION STATISTICS

	VSF(Our method)	k-NN regression	GP regression
Avg $\|\hat{\tau}-\tau\|_2$ (N/m)	0.504 $\pm$ 0.392	5.164 $\pm$ 4.812	6.037 $\pm$ 3.098
Max $\|\hat{\tau}-\tau\|_2$ (N/m)	1.405 $\pm$ 0.392	11.980 $\pm$ 3.646	7.727 $\pm$ 3.602
Avg $\|\hat{\tau}-\tau\|_2/\|\tau\|_2$	0.150 $\pm$ 0.117	1.302 $\pm$ 1.655	1.481 $\pm$ 1.838
Max $\|\hat{\tau}-\tau\|_2/\|\tau\|_2$	0.434 $\pm$ 0.207	5.351 $\pm$ 5.030	6.317 $\pm$ 3.640

the plant with the same end-effector pose but different joint configurations. We touch the plant from 11 different configurations and collect 400 joint angles and torques measurements in each touch. To evaluate our method, we take a k-fold cross validation approach. We use each trajectory as the test sequence and estimate a volumetric stiffness field from the remaining 10 trajectories. Note that we do not update the stiffness estimation while evaluating on the test sequence.

We compare our method to two baseline methods. k-nearest neighbors (k-NN) regression finds $N = 50$ nearest neighbors using the joint angles and predict torques as a RBF kernel weighted sum of neighbors' torques. Gaussian Process(GP) regression predicts joint torques from joint angles using an RBF kernel.

Evaluation metrics: We denote predicted torques as $\hat{\tau}$ and the ground truth torques as τ. We measured both the absolute torque prediction error $\|\hat{\tau} - \tau\|_2$ and the relative torque prediction error $\|\hat{\tau}-\tau\|_2/\|\tau\|_2$. The relative torque prediction error is recorded when $\|\tau\|_2 \geq 1$ Nm, which indicates the arm has touched the plant. We compute the average and maximum error in each sequence and report the mean and standard deviation of error over the 11 sequences in I.

Results: Our method has consistently smaller prediction error compared to the baseline methods as shown in Table I. By explicitly modeling a stiffness field, we can accurately predict joint torques when the robot arm touches the same location. The performance of the baseline methods shows that directly using similarity to previously observed joint angles is insufficient to predict joint torques. We also plot the changes of torque prediction error in one test trajectory in Fig. 3.

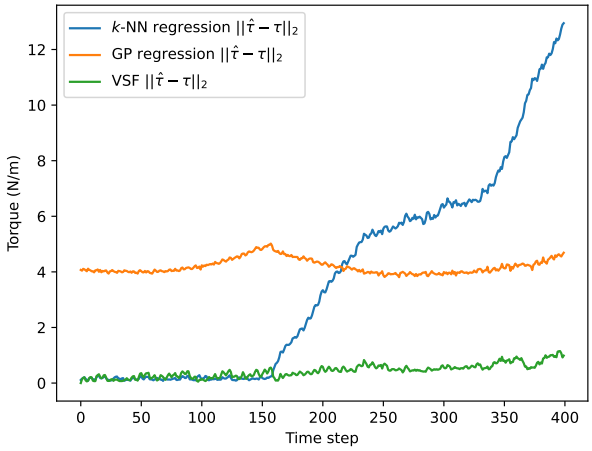

Fig. 3. Torque prediction error by different methods in one test trajectory.

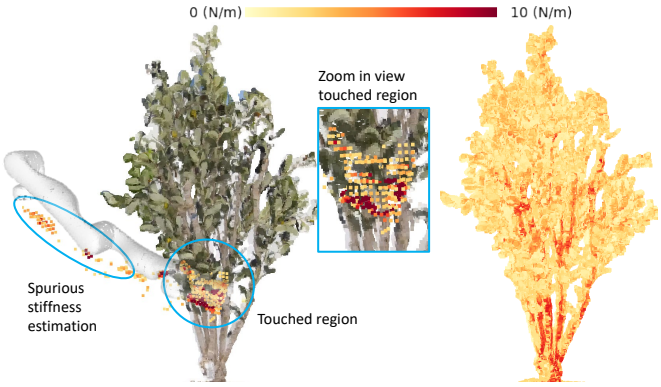

Fig. 4. Visualizing qualitative stiffness field estimation. The color bar at the top indicates the predicted stiffness. Left figure shows raw estimation of points with stiffness greater than 2 N/m. There is spurious stiffness estimation because of estimation ambiguity from limited number of touches. Right figure shows stiffness prediction to every point in the plant using color correlation.

B. Stiffness extrapolation

Although our technique builds a stiffness map in a relatively uninformed and localized manner, we consider how a small number of touches can be used to generalize across the unexplored volume. Certainly, touching the object all over to obtain a complete stiffness map would be time-consuming. We examine a possible approach that uses correlations in visual features to perform this generalization. Here we take only a single depth image of the artificial plant before touches happen. The left part of Fig. 4 shows raw stiffness map obtained from 8 touches to similar locations on the plant. The configuration of the arm is shown as transparent in the figure. The raw stiffness map has spurious stiffness estimation in the free space, because of limited number of touches from similar configurations.

For each point in the point cloud point we look up the stiffness values of nearby touched voxels, creating a dataset that maps RGB value to estimated stiffness. For all untouched points, we use k-NN regression to predict the stiffness value from the color. We use $k = 50$ neighbors and an RBF kernel. From Fig. 4 right, we can see qualitatively that even with this relatively naïve approach, the stiffness predictions align with our intuition that branches should be stiffer than leaves. In our future work, we are interested in exploring how other features of the neighborhoods of each point can be used to better generalize stiffness estimates across the whole object.

IV. CONCLUSION

In this paper, we introduce VSF, a new deformable object stiffness model which can be estimated online using an EKF. Our real world experiments show an estimated VSF can be used to predict joint torques when the same location is touched. We also show the VSF estimated from a small number of touches can be extrapolated to untouched regions using color correlation.

REFERENCES

[1] C.-A. Smarr *et al.*, "Domestic robots for older adults: Attitudes, preferences, and potential," *Int. J. Social Rob.*, vol. 6, pp. 229–247, 2014.

[2] E. Kayacan, Z. Zhang, and G. Chowdhary, "Embedded high precision control and corn stand counting algorithms for an ultra-compact 3d printed field robot," in *Robotics: Science and Systems*, 2018.

[3] A. Jain, M. D. Killpack, A. Edsinger, and C. C. Kemp, "Reaching in clutter with whole-arm tactile sensing," *Int. J. Robotics Research*, vol. 32, no. 4, pp. 458–482, 2013.

[4] B. Frank, C. Stachniss, R. Schmedding, M. Teschner, and W. Burgard, "Learning object deformation models for robot motion planning," *Robotics and Autonomous Systems*, vol. 62, no. 8, pp. 1153–1174, 2014.

[5] V. E. Arriola-Rios, P. Guler, F. Ficuciello, D. Kragic, B. Siciliano, and J. L. Wyatt, "Modeling of deformable objects for robotic manipulation: A tutorial and review," *Frontiers in Robotics and AI*, vol. 7, 2020.

[6] B. Frank, R. Schmedding, C. Stachniss, M. Teschner, and W. Burgard, "Learning the elasticity parameters of deformable objects with a manipulation robot," in *IEEE/RSJ Int. Conf. Intel. Robots and Systems (IROS)*, 2010, pp. 1877–1883.

[7] V. E. Arriola-Rios and J. L. Wyatt, "A multimodal model of object deformation under robotic pushing," *IEEE Transactions on Cognitive and Developmental Systems*, vol. 9, no. 2, pp. 153–169, 2017.

[8] S. Caccamo, P. Güler, H. Kjellström, and D. Kragic, "Active perception and modeling of deformable surfaces using gaussian processes and position-based dynamics," *IEEE-RAS Int. Conf. Humanoid Robots*, pp. 530–537, 2016.

[9] Y. Zhu, K. Lu, and K. Hauser, "Semi-empirical simulation of learned force response models for heterogeneous elastic objects," in *IEEE Int. Conf. Robotics and Automation (ICRA)*, 2020, pp. 1646–1652.

[10] L. Manuelli and R. Tedrake, "Localizing external contact using proprioceptive sensors: The contact particle filter," in *IEEE/RSJ Int. Conf. Intel. Robots and Systems (IROS)*, 2016, pp. 5062–5069.

[11] T. Pang and J. Umenberger, "Identifying external contacts from joint torque measurements on serial robotic arms and its limitations," *IEEE Int. Conf. Robotics and Automation*, pp. 6476–6482, 2021.

[12] B. Saund, S. Choudhury, S. S. Srinivasa, and D. Berenson, "The blindfolded robot: A bayesian approach to planning with contact feedback," in *ISRR*, 2019.

[13] J. Bimbo, A. S. Morgan, and A. M. Dollar, "Force-based simultaneous mapping and object reconstruction for robotic manipulation," *IEEE Robotics and Automation Letters*, vol. 7, pp. 4749–4756, 2022.